IBRO Reports 7 (2019) 70–79

Contents lists available at ScienceDirect

IBRO Reports

journal homepage: www.elsevier.com/locate/ibror

Research paper

Microglial response patterns following damage to the zebrafish olfactory bulb

Susanna R. Var, Christine A. Byrd-Jacobs*

Western Michigan University, Kalamazoo, Michigan, 49008-5410 USA

ARTICLE INFO

Keywords:
Microglia
Immune response
Deafferentation
Direct lesion
Olfactory bulb
Zebrafish

ABSTRACT

The inherent plasticity of the zebrafish olfactory system serves as a useful model for examining immune cell responses after injury. Microglia are the resident immune cells of the CNS that respond to damage by migrating to the site of injury and phagocytizing neuronal debris. While the olfactory system is renowned for its ability to recover from damage, the specific mechanisms of microglial involvement in olfactory system plasticity are unknown. To approach the potentially time-dependent effects of microglial activation after injury, we performed a time course analysis of microglial response profiles and patterns following different forms of damage: deafferentation by cautery ablation of the olfactory organ, deafferentation by chemical ablation of the olfactory epithelium, and direct lesioning of the olfactory bulb. Our aim was to demonstrate that immunocytochemistry and microscopy methods in zebrafish can be used to determine the timing of distinct microglial response patterns following various forms of injury. We found that permanent and temporary forms of damage to the olfactory bulb resulted in different microglial response profiles from 1 to 72 h after injury, suggesting that there may be critical timepoints in which microglia are activated that contribute to tissue and neuronal repair with a regenerative outcome versus a degenerative outcome. These distinctions between the different forms of damage suggest temporal changes relative to the potential for regeneration, since cautery deafferentation is permanent and unrecoverable while chemical ablation deafferentation and direct lesioning is reversible and can be used to observe the microglial relationship in neural regeneration and functional recovery in future studies.

1. Introduction

Microglia, the resident immune cells of the CNS, show a high degree of plasticity, and their ability to transform rapidly from a resting sensorial cell to active phagocytic state is well described (Davalos et al., 2005; Nimmerjahn et al., 2005; Morrison and Filosa, 2013). Increasing evidence has demonstrated that microglia also act as key modulators in neuronal development and plasticity, supporting and shaping brain tissue, distinct from other phagocytes that primarily function in innate immunity (Tremblay et al., 2010; Schafer et al., 2012; Hong et al., 2016). Under particular disease states or injury conditions, peripheral immune cells also travel to the CNS, migrating through blood vessels and cranial nerves to provide additional clearing of debris (Reemst et al., 2016; Ginhoux et al., 2010; Shechter et al., 2013).

The interaction between the nervous and immune systems affects both development across lifespan and recovery after injury and disease (Streit et al., 2009; Kumar and Loane, 2012). Brain disease and injury involve the activation of resident and peripheral immune cells to clear damaged and dying neurons (van Ham et al., 2014v). The recruitment and activation of immune cells is followed by phagocytosis, a key response to tissue damage that enables control of inflammation and tissue repair. The phagocytic behavior of immune cells is potentially important in the establishment of new axonal connections, as degenerating connections first must be removed for this event to occur (David and Kroner, 2011; Harry and Kraft, 2012).

Recent studies suggest the possibility that inadequate recruitment of monocyte-derived macrophages to the brain after injury results in incomplete functional recovery in mice (Wattananit et al., 2016). Currently it is not certain whether phagocytosis and the resolution of inflammation is dependent on the timely recruitment and migration of immune cells in order to lead to functional recovery in the brain. It is also unclear which immune cells are involved in the brain recovery process after injury, particularly in the olfactory system, an area of continually developing, high neuronal turnover.

The regenerative nature of the zebrafish is useful for examining the potential of the brain to recover from damage, and the constitutive neurogenesis of the olfactory system makes it an ideal model for regeneration studies. Zebrafish olfactory sensory neurons (OSN)s are

Abbreviations: OSN, olfactory sensory neuron; ir, immunoreactive

* Corresponding author at: Western Michigan University, Kalamazoo MI 49008-5410, USA.

https://doi.org/10.1016/j.ibror.2019.08.002
Received 19 March 2019; Accepted 23 August 2019

continually renewed, and new olfactory bulb neurons are generated throughout life (Byrd and Brunjes, 2001; Grandel et al., 2006; Brann and Firestein, 2014). The inherent plasticity of the zebrafish olfactory system is comparable in structure to most vertebrates and is easy to manipulate. For example, intranasal infusion of the detergent Triton X-100 causes rapid degeneration and regeneration of OSNs by 5 days and olfactory bulb reinnervation within 7 days following, resulting from a high turnover rate of both neuronal and non-neuronal elements (Iqbal and Byrd-Jacobs, 2010; White et al., 2015). This well-defined recovery model makes the zebrafish olfactory system ideal for examining the potential role of microglia in regeneration after injury.

Overactivation of microglia has been shown to cause neuronal dysfunction and disease in mammals (Brown and Neher, 2012; Silverman et al., 2016). Zebrafish microglia have dynamic processes that can respond to injury or infection by migrating to the site and phagocytizing pathogens and neuronal debris (Herbomel et al., 1999, 2001; Peri and Nüsslein-Volhard, 2008). It is possible that, with the proliferative capacities of zebrafish to repair lesions, there is a critical time period in which activation of microglia in this animal is ameliorative rather than damaging (Carrillo et al., 2016; de Preux Charles et al., 2016). To approach the potentially time-dependent effects of microglial activation, we performed a time course analysis of the microglial response profiles and patterns following different forms of damage: deafferentation by cautery ablation of the olfactory organ, deafferentation by chemical ablation of the olfactory epithelium, and direct lesioning of the olfactory bulb. This study aims to demonstrate that microscopy methods in zebrafish can be used to determine the location and timing of potentially distinct microglial response patterns following various forms of injury. Understanding the control of immune cell behavior in the highly plastic olfactory system could potentially lead to development of therapeutic methods for functional recovery after neuronal damage.

2. Materials and methods

2.1. Study cohort

Adult zebrafish, *Danio rerio*, were purchased from local commercial sources. Fish were maintained in 15-gallon aquaria filled with aerated, conditioned water at 28.5 °C and fed commercial flake food (Tetra) twice daily, each morning and afternoon. All experiments were conducted on adult zebrafish of both sexes that were 3 months of age or older and between 3–4.5 cm in length. Procedures were approved by the Institutional Animal Care and Use Committee. All possible efforts were made to minimize animal suffering and the numbers of animal used.

2.2. Deafferentation by cauterization of the olfactory organ

Olfactory bulbs were damaged by permanently and completely ablating the right olfactory organ via cautery (Fig. 1A). For this procedure, treated fish (n = 35) were anesthetized with 0.03% ethyl 3-aminobenzoate methanesulfonate salt (MS222, Sigma St. Louis, MO, USA), and the right olfactory organ was ablated using a small-vessel cautery iron as described previously (Byrd, 2000). The left olfactory organ was not treated to serve as an internal control. Control fish (n = 6) were anesthetized in the same manner but received no cautery damage. The same group of controls was used for all treatment groups. Treated fish were then transferred to a recovery tank before being returned to the aquarium for a survival period of 1, 4, 12, 24, 48, or 72 h.

2.3. Deafferentation by chemical ablation with Triton X-100

Olfactory bulbs were damaged by partial, temporary chemical ablation of the sensory epithelium through intranasal irrigation with a detergent solution (0.7% Triton X-100 with 0.15% methylene blue for visualization in 0.1 M phosphate-buffered saline, PBS) into the right olfactory organ (Fig. 1B). Treated fish (n = 31) were anesthetized with 0.03% MS222, and a pulled-glass wiretrol capillary tube was used to irrigate approximately 1 µl of the detergent solution inside the right excurrent naris as described previously (Iqbal and Byrd-Jacobs, 2010). The left olfactory organ was not treated to serve as an internal control. Control fish (n = 6) were anesthetized but received no intranasal irrigation. The same group of controls was used for all treatment groups. Treated fish were placed in a recovery tank before being returned to the aquarium for a survival period of 1, 4, 12, 24, 48, or 72 h.

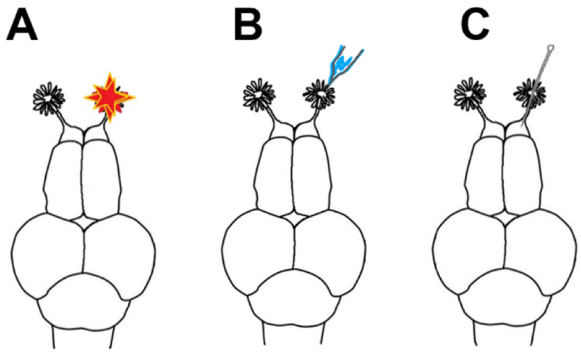

Fig. 1. Deafferentation and damage models used in treatment groups.
Dorsal view illustrations of treatments used on zebrafish brains. A) Permanent deafferentation of the olfactory bulb was performed by cauterization of the right olfactory organ. B) Temporary deafferentation of the olfactory bulb was performed by chemical ablation through intranasal irrigation with a detergent solution in the right olfactory organ. C) A direct lesion was performed by brief insertion and removal of an insect pin into the right olfactory bulb.

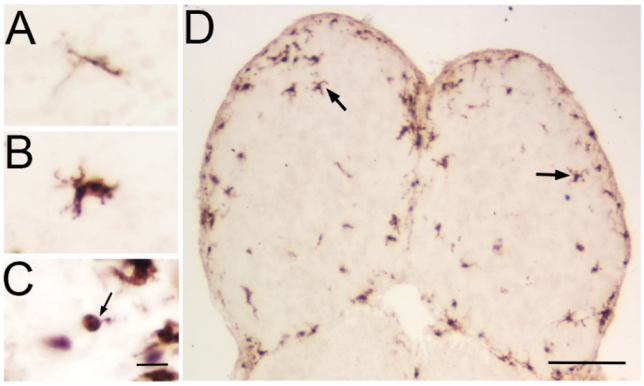

Fig. 2. Microglial morphologies in the olfactory bulb.
Microglia in the olfactory bulbs can transform from a “ramified, resting” sensorial cell (A) through a “transitioning” morphology (B) to an “amoeboid, actived" phagocytic state (C, arrow) in 3 types of morphologies evident with 4C4 labeling. Olfactory bulbs of an untreated control fish (D) labeled with 4C4 antibody showed comparable levels of 4C4-ir in both olfactory bulbs, and most profiles exhibited the ramified morphology (arrows). Scale bar = 20 µm for A, B, C; 100 µm for D.

2.4. Direct lesioning of the olfactory bulb

Olfactory bulbs were damaged by directly lesioning the right olfactory bulb with a stab wound (Fig. 1C). Treated fish (n = 32) were anesthetized with 0.03% MS222, and the right olfactory bulb was lesioned through a brief insertion and removal of 0.20 mm insect pin horizontally through the olfactory organ and the foramen in the cribriform plate and into the right olfactory bulb. The left side was not treated to serve as an internal control. Control fish (n = 6) were anesthetized but received no lesion. The same group of controls was used for all treatment groups. Treated fish were then transferred to a

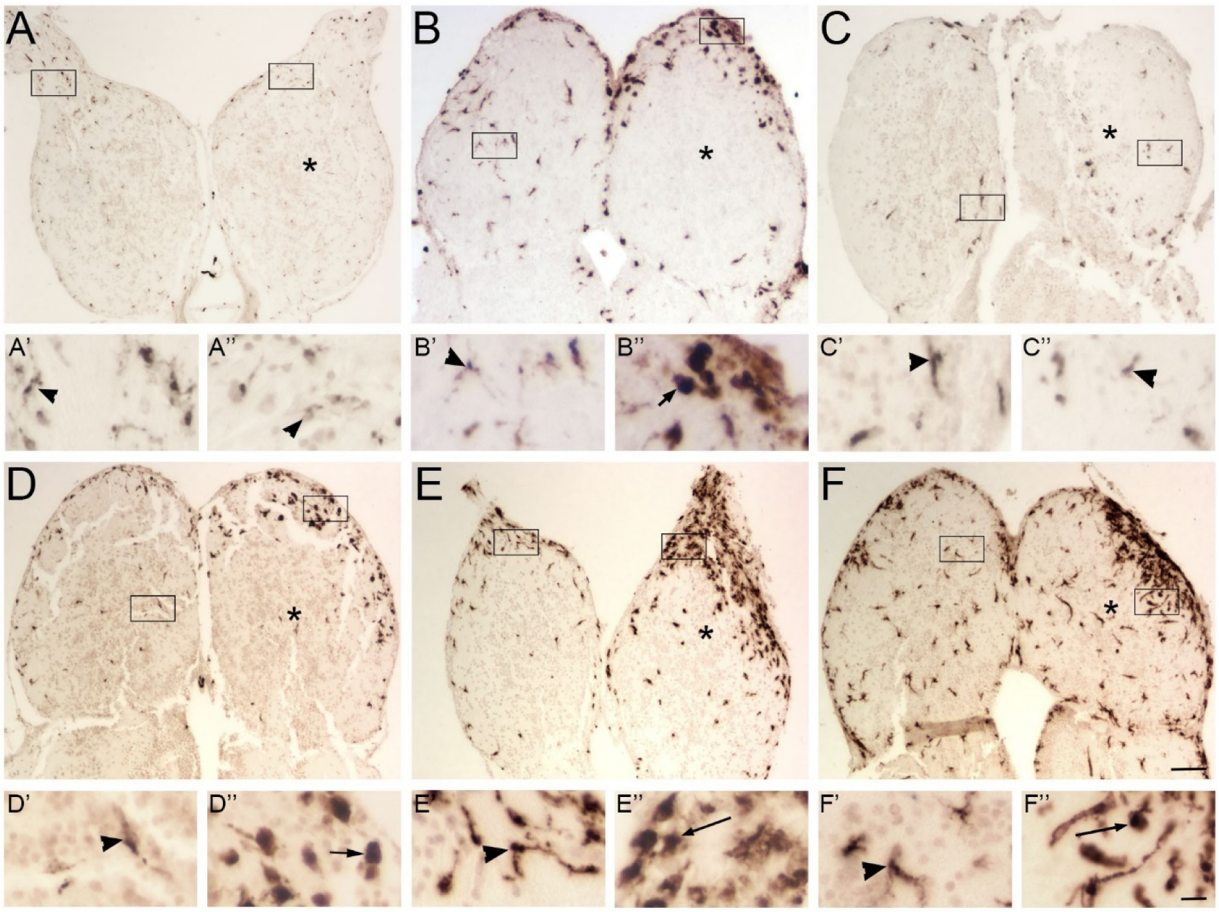

Fig. 3. Patterns of 4C4-ir microglial profiles after deafferentation by cautery.
Olfactory bulbs after deafferentation by cautery of the right olfactory organ were labeled with 4C4. Boxes indicate areas magnified in A'-F". A) At 1 h, there was no apparent difference in distribution of 4C4-ir profiles between the left, internal control and right, deafferented (*) olfactory bulbs. The few 4C4-ir profiles had a ramified (arrowheads) morphology in both the left (A') and right (A") bulbs. B) At 4 h, there was a substantial increase in 4C4-ir profiles in the injured bulb (*). In the intact bulb, labeled profiles were ramified (B'), while on the deafferented side, most 4C4-ir profiles showed an amoeboid (arrow) morphology (B"). C) At 12 h, the tissue appeared to be inflamed, and there were fewer 4C4-ir profiles in both olfactory bulbs than the previous timepoint. Most labeled profiles were of the ramified morphology in the intact (C') and the damaged (C") bulbs. D) At 24 h, there was another increase in 4C4-ir profiles in the deafferented bulb (*). While the intact bulb (D') continued to exhibit ramified microglia, the deafferented bulb (D") showed more amoeboid microglia. E) At 48 h, there were even more 4C4-ir profiles in the deafferented bulb (*), and while the intact bulb showed ramified microglia (E') the affected bulb displayed many amoeboid and transitioning (long arrows) morphologies (E"). F) At 72 h, the total level of microglia continued to increase in the deafferented bulb (*). The intact bulb had ramified cells (F'), while the deafferented bulb showed mostly microglia with the transitioning morphology (F"). Scale bar = 200 μm for A–F; 20 μm for A'-F".

recovery tank before being returned to the aquarium for a survival period of 1, 4, 12, 24, 48, or 72 h.

2.5. Immunohistochemistry

After the respective survival periods, fish were euthanized with 0.03% MS222, perfused transcardially with PBS, and then immersed in 4% paraformaldehyde for 24 h at 4 °C. Following dissection, tissues were rinsed in PBS, dehydrated in an ascending ethanol and xylene series of washes, and then embedded in paraffin for sectioning. Horizontal, semi-serial, 10 μm sections were mounted on positively charged slides.

Mounted sections were dewaxed and rehydrated before antigen retrieval for 10 min in sodium citrate solution at 100 °C, rinsing in PBS, and then placing in 3% H_2O_2 solution for 10 min to remove endogenous peroxidases. Sections were rinsed in PBS and placed in blocking solution (3% normal goat serum, 0.4% Triton X-100 in PBS) for 1 h at room temperature and in 4C4 mouse monoclonal antibody (1:100, a kind gift of Drs. Pamela Raymond and Peter Hitchcock, University of Michigan) to label microglia (Becker and Becker, 2001; Raymond et al., 2006; Craig et al., 2008; Baumgart et al., 2012; Tsarouchas et al., 2018). Sections were rinsed in PBS and then incubated in biotinylated goat anti-mouse secondary antibody (1:200, Vector Laboratories, Burlingame, CA, USA) for 1 h at room temperature. Following PBS rinses, sections were immersed in avidin-biotin-peroxidase solution (ABC Vectastain Elite, Vector Laboratories) and reacted with diaminobenzidine solution (Vector Laboratories) for about 6 min. Mounted sections were dehydrated and coverslipped with DPX mounting medium (Aldrich, St. Louis, MO, USA). Slides were then visualized with a Nikon Eclipse 80i microscope.

2.6. Quantification of microglia

4C4-immunoreactive (ir) profiles in both left and right olfactory bulbs were manually quantified at 400 × . For each fish, 3 sections that were 40 μm apart and displayed remnants of the olfactory nerve—the approximate area where injury occurred—were quantified and averaged for each fish. 4C4-ir profiles were also categorized by morphological characteristics as being ramified, transitioning, or amoeboid. Morphological criteria by Jonas et al. (2012) was used to establish these categories, where morphology classification of 1A, 2A, 1R, and 2R were considered ramified, 3A, 4A, 3R, and 4R were considered transitioning,

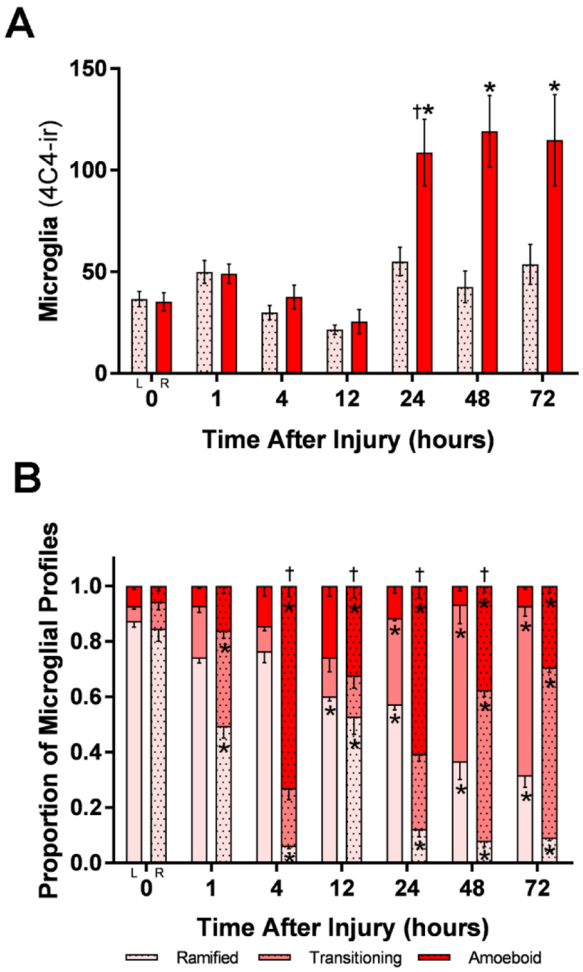

Fig. 4. Quantification of 4C4-ir profiles after deafferentation by cautery. A) Total microglia after cautery deafferentation showed significant increases in number of 4C4-ir profiles in the right (R) bulb at 24, 48, and 72 h compared to control fish, t = 0 h. B) 4C4-ir profiles after cautery deafferentation showed significantly different microglial morphologies with comparisons to control and between timepoints after injury. In the deafferented (R) bulb, amoeboid profiles significantly increased between 1–4 h, decreased between 4–12 h, increased at 12–24 h, and decreased again at 24–48 h in the right olfactory bulb. Transitioning profiles increased from control levels in the right (R) bulb at 1 h, 48 h, and 72 h. Ramified profiles showed a reduction from control levels at all timepoints. At 4–48 h, counts were different from the previous timepoint, showing the dynamic nature of the response. * = $P < 0.05$ compared with controls, † = $P < 0.05$ compared to the previous timepoint.

and 5A, 6A, 5R, and 6R were considered activated. We defined microglia of ramified morphology as having a small soma and greater than 3 processes with several secondary and tertiary branches; transitioning morphology possessed a larger soma with 3 or few processes that appeared thicker when compared to the ramified morphology; and amoeboid morphology possessed a large soma with few to no projections. To account for sample variance, comparisons between the proportion of different microglial morphologies within a sample were converted to percentages of the total number of microglia.

2.7. Statistical analysis

Analysis of 4C4-ir morphological profiles in both left and right olfactory bulbs were compared between timepoints within treatment groups using paired t-tests or Analysis of Variance (ANOVA) with Tukey's test for multiple class comparisons. P-values less than 0.05 were considered significant. All statistical analysis was performed using R statistical software (ver 3.2.3) and Graphpad Prism Software (ver. 7.03).

3. Results

Responsive microglia following unilateral injury were examined by quantifying 4C4-ir profiles in the olfactory bulbs. 4C4-ir microglial profiles were then categorized by microglial morphology to determine their activation state (Fig. 2A-C). The median size of fish was 3.3 cm. There were no significant differences between control and treated fish in labeling or profile distribution in relation to size and sex of fish.

3.1. Patterns of 4C4-ir microglial profiles after olfactory bulb deafferentation by cautery

Permanent, complete deafferentation of the olfactory bulb was achieved through unilateral ablation of the olfactory organ with a cautery iron. Distribution and amount of 4C4 labeling in both olfactory bulbs were compared to that in intact control fish, which showed comparable levels of ramified 4C4-ir profiles in both the olfactory bulbs (Fig. 2D). At 1 h following cautery deafferentation, there was no obvious difference in microglial profiles in the ipsilateral or contralateral bulbs (Fig. 3A), and the microglial morphologies appeared similar in both bulbs (Fig. 3A', A"). At 4 h, there was a substantial increase in 4C4-ir profiles observed in the damaged right olfactory bulb (Fig. 3B). The microglia appeared to change from ramified to amoeboid morphologies in the affected bulb (Fig. 3B', B"). At 12 h, there appeared to be more ramified 4C4-ir profiles but a decrease in total 4C4-ir profiles in both bulbs (Fig. 3C, C', C"). The right olfactory bulb also appeared to be inflamed at this timepoint, as evidenced by cracks in the sections. Both total 4C4-ir profiles as well as activated 4C4-ir profiles appeared to increase again in the deafferented bulb at 24 h (Fig. 3D, D', D"). At 48 h, there was extensive 4C4 labeling in the ipsilateral bulb (Figure E), and many immunoreactive profiles displayed the transitioning morphology (Figure 3E', E"). By 72 h, the level of 4C4-ir profiles remained high in the deafferented bulb (Fig. 3F), particularly in the transitioning morphology (Fig. 3F', F").

Quantification of total microglia after cautery deafferentation showed significant increases in 4C4-ir profiles in the right, deafferentated olfactory bulb at 24, 48, and 72 h compared to control bulbs of untreated fish, t = 0 h (Fig. 4A). There were no significant differences between the number of 4C4-ir profiles in the control bulbs and left internal control bulbs of treated fish. Examination of the number of 4C4-ir profiles 5 and 7 days after injury showed no significant differences compared to control (data not shown). Quantification of total 4C4-ir microglial profiles after deafferentation by cautery showed significantly different morphologies between different times after injury (Fig. 4B). Comparisons to control bulbs showed that there were significantly decreasing ramified profiles 4–72 h after injury in both the ipsilateral and contralateral bulbs. Amoeboid profiles significantly increased at 4, 12, 24, 48, and 72 h after injury in the ipsilateral bulb compared to control bulbs; additionally, comparisons between timepoints showed that amoeboid profiles significantly increased between 1–4 h, decreased between 4–12 h, increased again between 12–24 h, and finally decreased again between 24–48 h in the damaged bulb following peripheral deafferentation. Transitioning profiles significantly increased at 1 h in the ipsilateral bulb, 24 h in the contralateral bulb, and 48 h and 72 h in both the ipsilateral and contralateral bulbs compared to control.

3.2. Patterns of 4C4-ir microglial profiles after olfactory bulb deafferentation by chemical ablation

Chemical ablation of the sensory epithelium of the right olfactory organ was performed with intranasal irrigation of detergent in order to achieve temporary deafferentation of the olfactory bulb. After 1 h, there appeared to be a small increase in 4C4-ir profiles in both deafferented and intact olfactory bulbs (Fig. 5A), with more amoeboid and transitioning microglia around the periphery but mostly ramified profiles

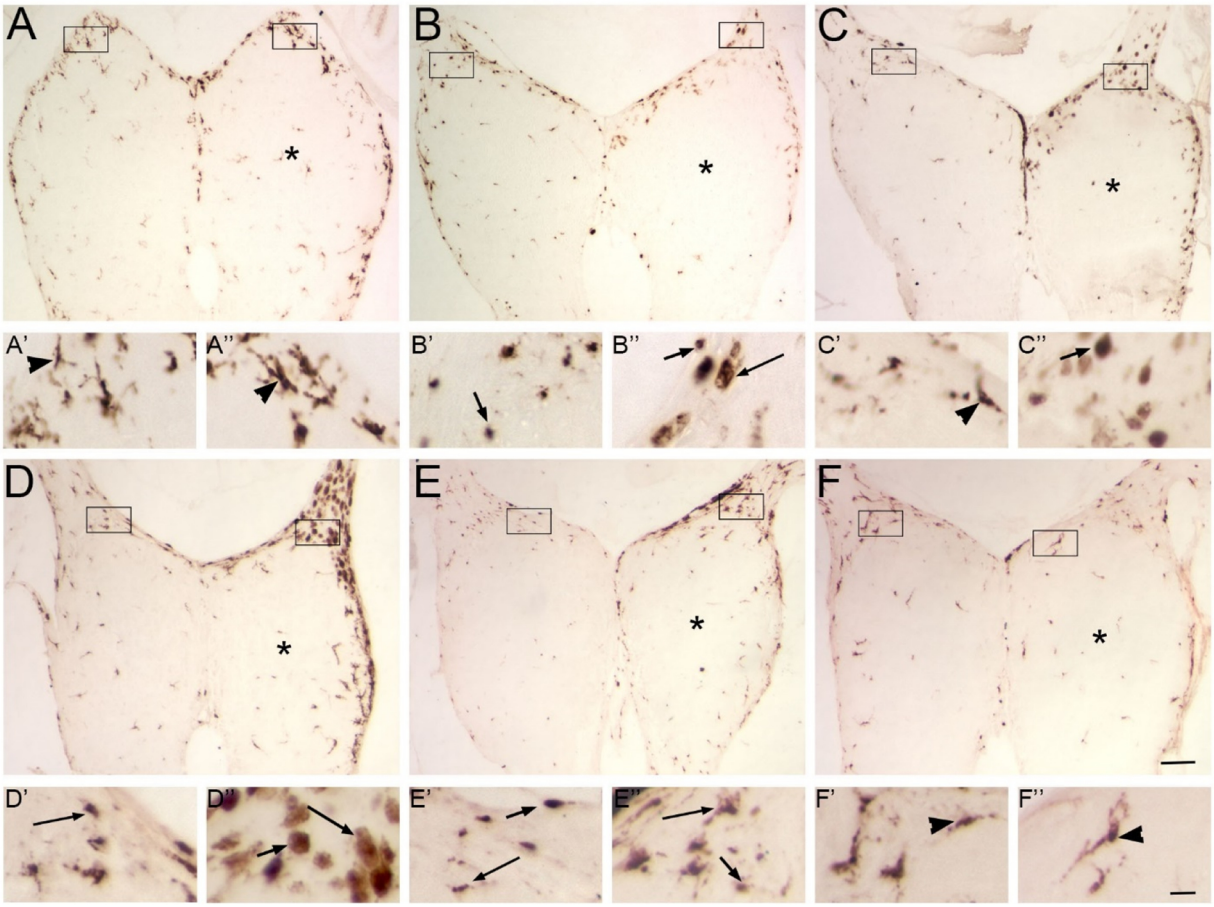

Fig. 5. Patterns of 4C4-ir microglial profiles after deafferentation by chemical ablation.
Olfactory bulbs deafferented by chemical ablation of the sensory epithelium of the right olfactory organ were labeled with 4C4. Boxes indicate areas magnified in A'-F". A) At 1 h, there appeared to be no difference in 4C4 labeling between left, intact and right, deafferented (*) bulbs. There was a small increase in ramified (arrowheads) microglial profiles around the periphery of both the intact (A') and deafferented (A") olfactory bulbs. B) At 4 h, there was still no obvious change in 4C4 labeling with deafferentation (*). There seemed to be more amoeboid (arrows) and transitioning (long arrow) in both olfactory bulbs (B', B"). C) At 12 h, there seemed to be more 4C4 profiles on the deafferented side (*), and there was a noticeable increase in amoeboid profiles in the right olfactory bulb (C") compared to the internal control side (C'). D) At 24 h, there appeared to be an increase in total number of microglia in the affected bulb (*); most of the profiles were in the olfactory nerve layer and were of the amoeboid and transitioning morphology (D', D"). E) At 48 h, the 4C4 profiles in the deafferented bulb (*) were localized to the olfactory nerve layer. Most profiles at this time point were transitioning or amoeboid in both olfactory bulbs (E', E"). F) At 72 h, the distribution of 4C4-ir profiles resembled control fish. Most labeled profiles continued to exhibit primarily the ramified morphologies (F', F"). Scale bar = 200 μm for A–F; 20 μm for A'-F".

labeled (Fig. 5A', A"). Amoeboid profiles continued to become more prominent after 4 h (Fig. 5B, B', B") and 12 h (Fig. 5C, C', C") in both bulbs, although there was no obvious change in total amount of 4C4 labeling. At 24 h, there seemed to be an increase in 4C4 labeling in the deafferented bulb (Fig. 5D), especially within and around the olfactory nerve. The 4C4-ir profiles were mostly of the ramified morphology in the intact bulb (Fig. 5D') and the amoeboid and transitioning morphologies in the deafferented bulb (Fig. 5D"). 4C4 labeling was minimal overall at 48 h, with an accumulation of immunoreactive profiles at the olfactory nerve (Fig. 5E), mostly displaying transitioning or amoeboid morphology in both bulbs (Fig. 5E', E"). The amount of 4C4 labeling continued to return to near-control levels by 72 h (Fig. 5F) and displayed primarily the ramified morphology (Fig. 5F', F").

Quantification of total 4C4-ir microglia after temporary deafferentation showed no significant differences compared to control (Fig. 6A). There were no significant differences between the number of 4C4-ir profiles in the control bulbs and left internal control bulbs of treated fish. Although there were changes in distributions and morphologies at various times after injury (Fig. 6B). There was a significant decrease in ramified profiles 1–72 h after injury in both the deafferented and intact olfactory bulbs (Fig. 6B). Amoeboid profiles significantly increased at 4, 12, 24, 48, and 72 h after injury in both olfactory bulbs, significantly increasing between 4–12 h, peaking at 12 h, and significantly decreasing between 12–24 h when comparisons were made in between each timepoint to observe changes throughout time after injury.

3.3. Patterns of 4C4-ir microglial profiles after direct lesioning

Direct lesions were performed by injuring the right olfactory bulb with a stab wound. There was small decrease in 4C4-ir profiles after 1 h in both bulbs, with very few 4C4-ir profiles observed (Fig. 7A). Those that were present were of the amoeboid or transitioning morphology in both intact (Figure A') and lesioned (Figure A") bulbs. There was a noticeable increase in 4C4-ir profiles in both the ipsilateral and contralateral bulbs following direct injury at 4 h (Fig. 7B). Most profiles were at the periphery of the bulbs and were amoeboid or transitioning morphologies (Fig. 7B', B"). At 12 h, there was an obvious increase in transitioning 4C4-ir profiles in the lesioned bulb (Fig. 7C), and the profiles appeared to accumulate along the path of the stab wound. In both intact (Fig. 7C') and lesioned (Fig. 7C") bulbs, the labeled microglia appeared to be transitioning between morphologies. 4C4-ir profiles decreased to near-control levels by 24 h (Fig. 7D) and remained at that level over 48 h (Fig. 7E) and 72 h (Fig. 7F). At all these times,

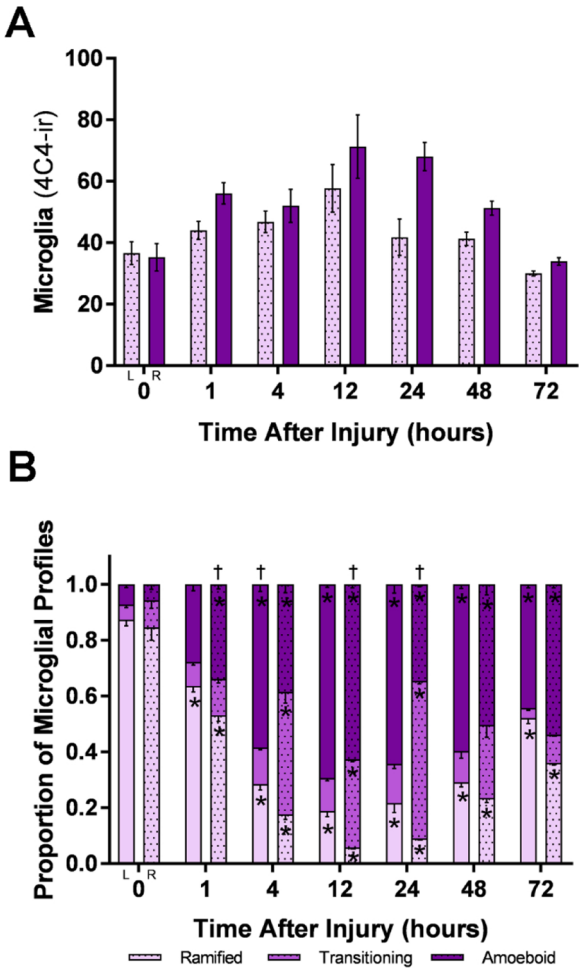

Fig. 6. Quantification of 4C4-ir profiles after deafferentation by chemical ablation.

A) Total microglia after temporary deafferentation showed no significant differences compared to control. B) A proportion of 4C4-ir profiles after temporary deafferentation showed significantly different microglial morphologies in the deafferented bulb (R) with comparisons to internal control (L) and intact controls (t = 0 h) and between timepoints after injury. Comparisons to control showed that there was a significant decrease in ramified profiles 1–72 h after injury in both olfactory bulbs. Amoeboid profiles significantly increased at timepoints after 4 h in both olfactory bulbs, significantly increasing between 4–12 h, peaking at 12 h, and significantly decreasing between 12–24 h. * = $P < 0.05$ compared with controls, † = $P < 0.05$ compared to the previous timepoint.

4C4-ir profiles displayed amoeboid or transitioning morphologies (Fig. 7E', E", F', F").

Quantification of total microglia after a direct lesion to the right olfactory bulb showed a significant decrease at 1 h in the contralateral bulb and a significant increase from 4 to 12 h in the ipsilateral bulb (Fig. 8A). There were no significant differences between the number of 4C4-ir profiles in the control bulbs and left internal control bulbs of treated fish, except at 1 h after injury, where there was a slight decrease in total 4C4-ir microglial profiles. Quantification of total 4C4-ir microglial profiles after direct lesioning showed significantly different 4C4-ir morphologies between different times after injury (Fig. 8B). Comparisons to control fish showed that there were significantly fewer ramified profiles at 1, 4, 12, 24, 48, and 72 h after injury in both the ipsilateral and contralateral bulbs. Amoeboid profiles significantly increased at 1 and 4 h in both the ipsilateral and contralateral bulbs compared to control fish. Comparisons between timepoints showed that amoeboid profiles significantly decreased between 4–12 h in both bulbs. Transitioning profiles significantly increased at 1, 12, 24, 48, and 72 h in both the ipsilateral and contralateral bulbs compared to control.

Heatmaps were generated for each experimental group to produce a visual overview of microglial profile distributions in the injury response to three different forms of bulb damage (Fig. 9). Deafferentation by cautery produced high to low levels of ramified profiles from 0 to 72 h, high levels of transitioning profiles from 24 to 72 h, and amoeboid profiles highest at 4 and 12 h in the ipsilateral bulb (Fig. 9A). Deafferentation by chemical ablation showed higher to lower levels of ramified profiles from 0 to 48 h, and increasing levels of transitioning profiles from 4 to 24 h, amoeboid profiles highest at 12 h in both OBs (Fig. 9B). Direct lesioning of the olfactory bulb had similar microglial profile patterns, in which ramified profiles were lowest at all times after damage, and amoeboid profiles increased from 1 to 4 h, while transitioning profiles increased from 12 to 72 h (Fig. 9C).

4. Discussion

In this study, we reported the microglial response patterns and timing following different forms of olfactory bulb damage, including permanent deafferentation by cautery, temporary deafferentation by chemical ablation, and stab wound by direct lesioning. We employed different forms of damage to the olfactory bulb because of the differential effects each type would have on the OSNs. This allowed us to observe whether the microglial response patterns differed between completely eliminating OSNs through permanent deafferentation, damaging only mature OSNs with the possibility of regeneration through temporary deafferentation, and injuring the OSNs and olfactory bulb cells directly through a direct lesion.

Previous studies in our lab investigated the short- and long-term effects on deafferentation of the olfactory bulb and its recovery. Cautery deafferentation procedures have been an effective method for examining the effects on the degeneration of the olfactory bulb (Byrd, 2000; Villanueva and Byrd-Jacobs, 2009), causing a complete, permanent deafferentation of the olfactory bulb (Scheib et al., 2019). Analysis showed that the olfactory organ was missing on the ablated side, leaving little potential for the olfactory bulb to regenerate. Additionally, loss of olfactory bulb volume continued to decrease for up to 6 weeks with a gradual reduction in total cell number in the bulb (Byrd, 2000), likely due to the rapid and substantial increase in cell death after complete ablation of the olfactory organ by cautery (Vankirk and Byrd, 2003). Further with this type of deafferentation, changes in dendritic structure are apparent throughout 8 weeks after permanent deafferentation (Pozzuto et al., 2019).

To examine the effects of long-term deafferentation and reafferentation of the olfactory bulb, our lab developed a novel method using repeated intranasal irrigation with Triton X-100 detergent. Infusion of the zebrafish olfactory organ with the detergent Triton X-100 causes a partial, temporary deafferentation of the olfactory bulb by killing most OSNs, followed by rapid regeneration of OSNs within five days (Iqbal and Byrd-Jacobs, 2010). Repeated infusion of the detergent every three days results in a severely damaged olfactory epithelium, reduced innervation of the olfactory bulb, and loss of olfactory-mediated behaviors (Paskin et al., 2011; Paskin and Byrd-Jacobs, 2012). Cessation of intranasal irrigation results in restoration of the olfactory epithelium, reinnervation of the olfactory bulb, complete return of glomerular distribution and odorant-mediated behavior, recovery of olfactory bulb volume number of tyrosine hydroxylase expression (Paskin et al., 2011; Paskin and Byrd-Jacobs, 2012; White et al., 2015). Similarly, continuous wax plug insertions into the naris affects the olfactory organ structure and reduces afferent input to the bulb, yet allows for recovery of glomeruli and axons and olfactory bulb reinnervation after cessation (Scheib et al., 2019).

A direct lesion through a stab wound is used to mimic a traumatic brain injury, a technique that has long been employed in zebrafish studies to examine their regenerative properties (März et al., 2011; Baumgart et al., 2012; Anand and Mondal, 2018; Cacialli et al., 2018).

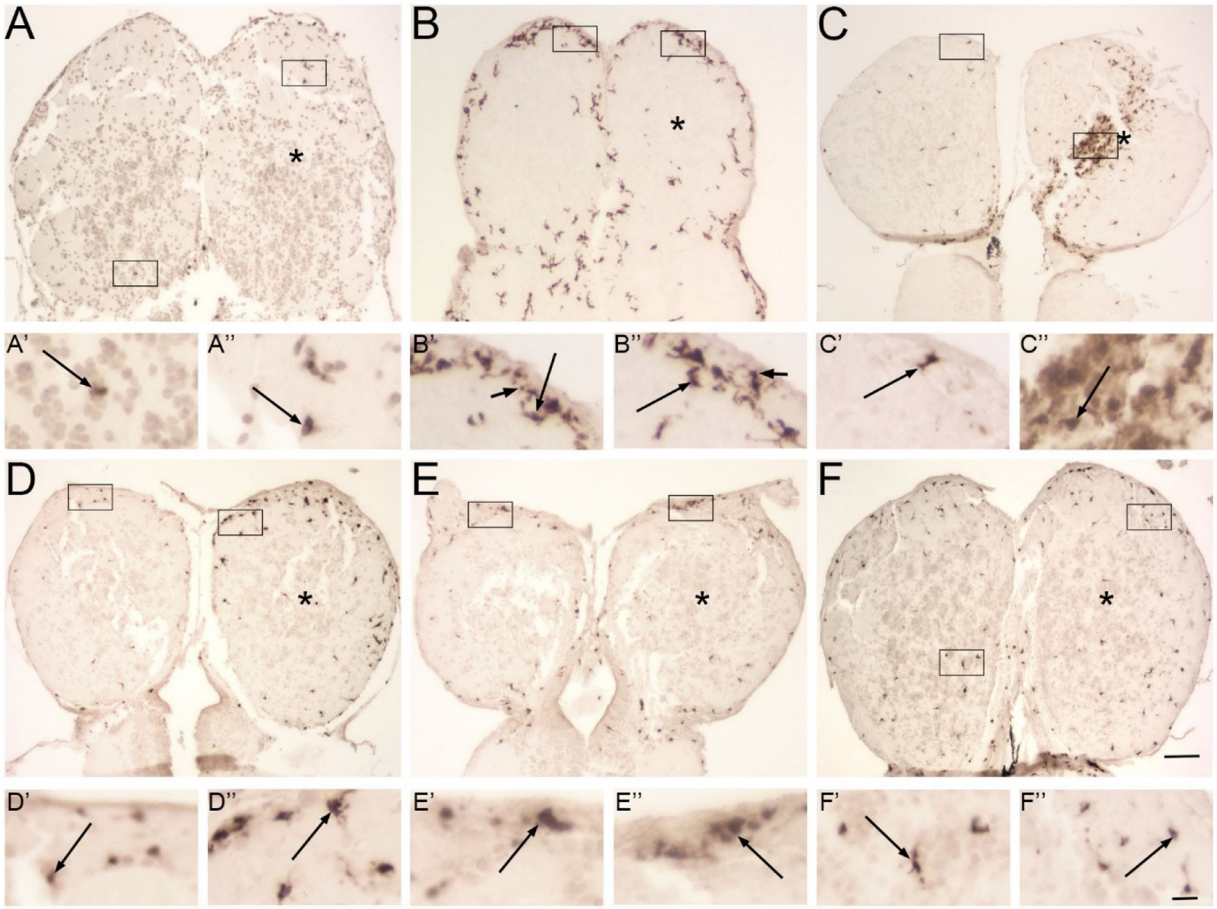

Fig. 7. Patterns of 4C4-ir microglial profiles after direct lesioning.
Olfactory bulbs after a direct lesion to the right olfactory bulb (*) and labeled with 4C4. Boxes indicate areas magnified in A'-F". A) At 1 h, there were very few 4C4-ir profiles in either bulb. The scant immunoreactive profiles were of the transitioning (long arrows) morphology in both intact (A') and lesioned (A") bulbs. B) At 4 h, there was a noticeable increase in labeled profiles in both bulbs, and most exhibited transitioning and amoeboid (arrows) morphologies in both olfactory bulbs (B', B"). C) At 12 h, there was an accumulation of labeled cells along the presumptive site of the wound. Higher magnification revealed transitioning profiles in the intact bulb (C'), and especially numerous in the lesioned olfactory bulb (C"). D) At 24 h, there were fewer 4C4-ir profiles and they were observed around the bulb periphery. In the intact bulb, profiles were few and of the transitioning morphology (D'); the lesioned bulb had many more 4C4 profiles, but they also were mostly the transitioning shape (D"). At 48 h (E) and 72 h (F), total microglial profiles slowly decreased to near-control levels (E', E", F', F") and exhibited mostly transitioning morphology. Scale bar = 200 μm for A–F; 20 μm for A'-F").

This is the first study to examine microglial activation patterns after a direct lesion. In this current study, we performed a time course to visualize these microglial patterns at specific timepoints after injury in the highly plastic olfactory system.

Different forms of olfactory bulb damage resulted in microglial activation patterns at specific timepoints that were distinct between the permanent and temporary forms of deafferentation. The microglial response patterns following cautery deafferentation resulted in specific, significant increases and decreases in amoeboid profiles in only the damaged olfactory bulb.Amoeboid profiles significantly increased at 4 h, decreased at 12 h, increased again at 24 h, and finally decreased again at 48 h. This pattern of response over time suggest that microglial activation may occur in two distinct recruitment phases: by 4 h after injury and again 12 h after injury. Previous studies have shown that an initial response through chemotactic upregulation occurs 4–6 h after injury in mammals (Calvo et al., 1996; Woodcock et al., 2017), corresponding with the initial activation of resident microglia and subsequent secretion of chemokines that lead to the CNS infiltration of blood-derived monocytes observed in several pathologies. We observed that the significant fluctuations of increasing and decreasing amoeboid profiles in the damaged bulb seen after cautery deafferentation at 12 h (decrease), and 24 h (increase), differed from the significant fluctuations of amoeboid profiles seen after chemical ablation deafferentation at 12 h (increase), 24 h (decrease).

Chemical ablation showed significantly different microglial morphologies between times after injury that were similar to cautery deafferentation but differed in temporal sequences. With chemical ablation, amoeboid profiles significantly increased at 4 h, peaked at 12 h, and significantly decreased between at 24 h in both the damaged and undamaged olfactory bulbs. At 24 h after damage, there were more transitioning profiles in the damaged bulb than in the undamaged bulb, resulting in proportionately less amoeboid profiles in the damaged bulb. These differences between these forms of deafferentations suggest temporal changes relative to severity of damage. This may play a role in the potential for regeneration, since cautery deafferentation is permanent and unrecoverable while chemical ablation deafferentation is reversible and can be used to observe the microglial relationship in neural regeneration and functional recovery in future studies.

Our use of a direct lesion injury is comparable to a traumatic brain injury, where the effects result in an increase in internal tissue damage. This form of damage resulted in a different microglial response pattern compared to cautery deafferentation, but was more comparable to the chemical ablation deafferentation, where both types of injuries are reversible and microglia in both the damaged and undamaged olfactory bulbs exhibited a noticeable response to the injury compared to controls. A major difference between chemical ablation and direct lesion

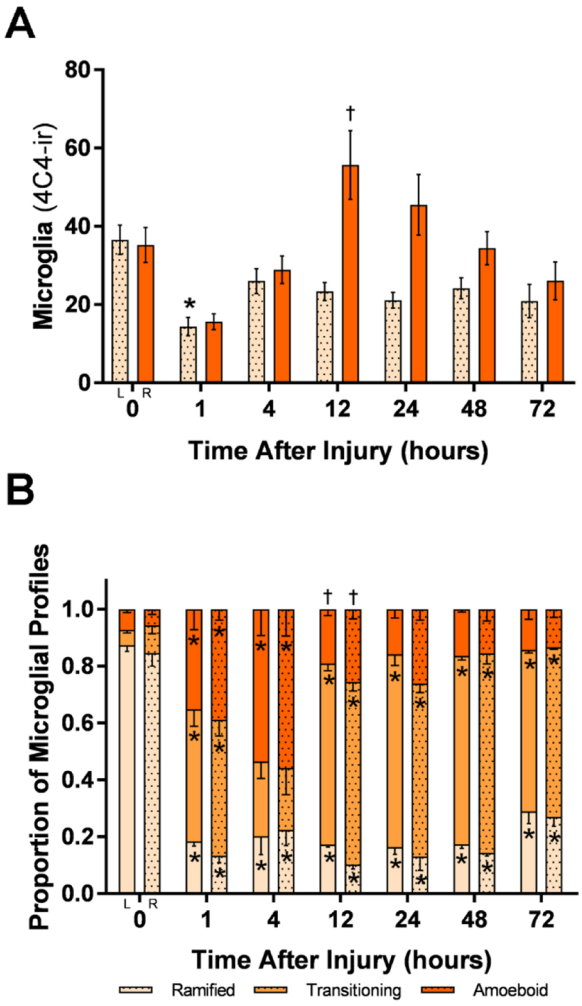

Fig. 8. Quantification of 4C4-ir profiles after direct lesioning.
A) Total microglia after a direct lesion to the right olfactory bulb (R) showed an apparent decrease that trended towards significance ($p = 0.07$) in the ipsilateral bulb and a significant increase in the contralateral bulb at 1 h. At 12 h, there was a significant increase in the ipsilateral bulb. B) 4C4-ir profiles after a direct lesion to the right olfactory bulb showed significantly different microglial morphologies with comparisons to control and between timepoints after injury. Amoeboid profiles significantly increased at 1 and 4 h and significantly decreased at 12 h in both olfactory bulbs. Transitioning profiles increased from 0 to 1 h and 4–72 h. Ramified profiles were significantly decreased at all timepoints after injury. * = $P < 0.05$ compared with controls, † = $P < 0.05$ compared to the previous timepoint.

was amoeboid profiles significantly decreasing between at 12 h in both the damaged and undamaged olfactory bulbs.

For all forms of olfactory bulb damage, we observed amoeboid microglial profiles significantly increasing 4 h after damage, with notable differences at 12 h after damage between the different injury types. Additionally, the left bulb was untreated and used as an internal control. While there were no significant differences between the intact side and treated side in the cautery and chemical ablation treatments, there were some effects on the contralateral side after a direct lesion. With this injury type, there may still be communication between both olfactory bulbs due to the diffusion of injury response factors, as a result of the increase in internal tissue damage and presence of superficial cellular debris. Treatment with Triton X-100 to the right olfactory bulb also displayed some small yet insignificant differences in the untreated left bulb; however, a olfactory bulb volume and glomerular analysis from a previous study demonstrated that the intact left olfactory bulb volume and glomeruli was unaffected after chemical lesioning (Paskin et al., 2011; White et al., 2015).

Cautery deafferentation exhibited a peculiar pattern compared to chemical and direct lesioning, the reversible forms of damage and deafferentation. Our observation of an increase in amoeboid profiles between 12 h and 24 h after cautery deafferentation in the damaged bulb, differed from the decrease in amoeboid profiles that we observed between 12 h and 24 h after temporary deafferentation and direct lesioning in both the olfactory bulbs. It is possible that the nature of the injury drives the prominent microglial morphology, where severity of injury and inflammation play role in the reconstitution of microglial cells. The decrease in amoeboid profiles that occurs between 4 h and 12 h after cautery deafferentation may be due to a delayed recruitment phase. A recent study reported anti-inflammatory cytokines, such as tgf-β1a and tgf-β3, being expressed at low levels during initial regeneration, and upregulated during late regeneration in zebrafish, suggesting a biphasic immune response within the 48 h after injury (Tsarouchas et al., 2018). Other studies have suggested that adult microglia have a low proliferation level and slow turn-over rate in mice (McCarthy and Leblond, 1988; Lawson et al., 1992; Inman and Downs, 2007), suggesting proliferation and reconstitution of microglia to be the limiting factor, perhaps exacerbated by the severity of the damage.

The rate of microglial proliferation or recruitment of cells from areas outside of the brain may be a limiting factor in the temporal microglial response to injury. Recent studies manipulating numbers of resident microglia suggest that microglial cells can be rapidly reconstituted by proliferation of resident cells, or by infiltrating monocytes (Varvel et al., 2012; Bruttger et al., 2015). In mice, the brain population of microglial cells are actively renewed and maintained by a sensitive balance of opposing forces: proliferation and apoptosis (Askew et al., 2017). In the healthy brain, mosaic-like organization of the microglial population cause processes of individual cells to avoid contact with one another, which is only disrupted with alterations of age, systemic factors, pathology, or injury (Gomez-Nicola and Perry, 2015). The primary temporal response seen in our study may be by resident microglia in the olfactory bulb. In peripheral tissue, pathogens and dead or dying cells are cleared by macrophages, which is followed by either programmed cell death or the exiting of the immune cells from the site of injury (Savill et al., 2002; Ravichandran and Lorenz, 2007; Murray and Wynn, 2011). Additionally, other studies have suggested that further amplification, a temporal factor, may be due to migration of microglia from other regions of the brain or peripheral macrophages entering through blood vessels and cranial nerves (Ransohoff and Perry, 2009; Shechter et al., 2013), possibly contributing to the secondary temporal phase of the response that occurs at 12 h after injury. To further respond to the damage, microglia may need time to proliferate or move from other areas of the brain, particularly areas lacking a blood-brain barrier, where microglia in these areas show a slightly different phenotype (Lawson et al., 1990; Mittelbronn et al., 2001); however, these processes are not understood in zebrafish.

Study limitations include variability in sample processing during insult procedures. Care was taken when performing the direct lesion injury without harming other parts of the brain yet still initiating a significant amount of damage for an immune cell response. If the direct lesion was not introduced properly, fish would be mortally wounded and die immediately after the procedure. Efforts to characterize fully the anatomical and functional phenotype of responding microglia have differed over the years. There are many approaches used for classifying the morphological change in microglia, but there is no gold standard. In this study, the morphological differences in microglia that are suggested to represent different functional states were analyzed by one individual to ensure consistency in visually identifying and distinguishing between the different morphologies and categorized based on size of soma and number of processes as characterized by Jonas et al., 2012.

In conclusion, we performed a time course analysis of microglial morphological patterns following different forms of injury in the highly

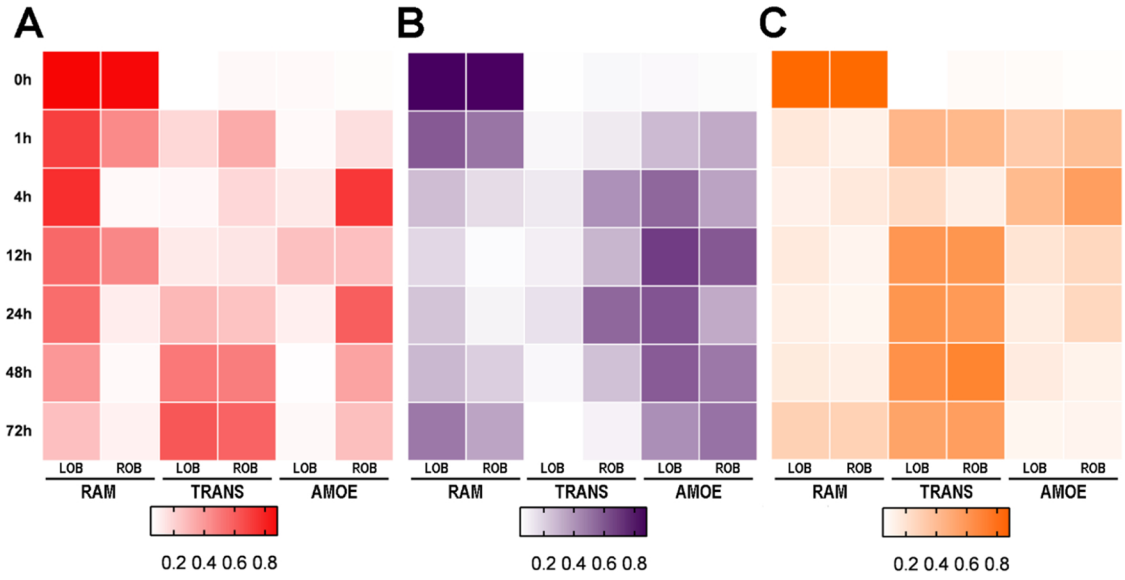

Fig. 9. Patterns of 4C4-ir microglial morphologies in different treatment groups.
Heatmaps were generated for each experimental group using Graphpad. A) Cautery deafferentation (red) showed darker to lighter ramified (RAM) profiles from 0 to 72 h, darker transitioning (TRANS) profiles from 24 to 72 h, and amoeboid (AMOE) profiles darkest at 4 and 12 h in the right olfactory bulb (ROB). B) Deafferentation by chemical ablation (purple) showed darker to lighter ramified profiles from 0 to 48 h, only moderate levels of transitioning profiles from 4 to 24 h, and amoeboid profiles darkest at 12 h in both olfactory bulbs. C) Direct lesioning (orange) showed similar microglial profile patterns, in which ramified profiles are lighter from 1 to 72 h, and darker amoeboid profiles increase from 1 h–4 h, while darker transitioning profiles increased from 12 to 72 h.

plastic olfactory system, and we demonstrated that microscopy methods in zebrafish can be used to determine the timing and localization of distinct microglial responses. These findings suggest that there may be critical timepoints in which microglia are activated that potentially can contribute to tissue and neuronal repair with a regenerative outcome versus a degenerative outcome. Cellular immune response is a prerequisite for tissue regeneration, just as inflammation is required for the regeneration of injured hearts in zebrafish (de Preux et al., 2016); however, the beneficial or determinantal effect of these immune cells is likely disease-dependent, as seen in mouse models (Ajami et al., 2011; Wattananit et al., 2016). It is important to note the high regenerative capacity of the zebrafish to restore tissue, notably brain and cardiac tissues (Kyritsis et al., 2012; Missinato et al., 2018; Shimizu et al., 2018); therefore, identifying conditions and relative timing of immune cell response that promote the regeneration of zebrafish neuronal tissue may provide insight on understanding the lower regenerative potential in mammals. Further studies are needed to assess the migratory or proliferation pattern of the microglial response as well as the role of microglia in potential neuroregeneration and functional recovery after damage to the olfactory bulb.

Conflicts of interest

The authors declare no conflict of interest.

Acknowledgements

We are very grateful to A. McKenna and Dr. D. Trimpe for their contributions to initial studies of this project. This work was supported financially by WMU funds (CBJ) and WMU graduate student research grant (SRV).

References

Ajami, B., Bennett, J.L., Krieger, C., McNagny, K.M., Rossi, F.M.V., 2011. Infiltrating monocytes trigger EAE progression, but do not contribute to the resident microglia pool. Nat. Neurosci. 14 (9), 1142–1149. https://doi.org/10.1038/nn.2887.

Anand, S.K., Mondal, A.C., 2018. TrkB receptor antagonism inhibits stab injury induced proliferative response in adult zebrafish (*Danio rerio*) brain. Neurosci. Lett. 672, 28–33. https://doi.org/10.1016/j.neulet.2018.02.040.

Askew, K., Li, K., Olmos-Alonso, A., Garcia-Moreno, F., Liang, Y., Richardson, P., Tipton, T., Chapman, M.A., et al., 2017. Coupled proliferation and apoptosis maintain the rapid turnover of microglia in the adult brain. Cell Rep. 18 (2), 391–405. https://doi.org/10.1016/j.celrep.2016.12.041.

Baumgart, E.V., Barbosa, J.S., Bally-cuif, L., Götz, M., Ninkovic, J., 2012. Stab wound injury of the zebrafish telencephalon: a model for comparative analysis of reactive gliosis. Glia 60 (3), 343–357. https://doi.org/10.1002/glia.22269.

Becker, T., Becker, C.G., 2001. Regenerating descending axons preferentially reroute to the gray matter in the presence of a general macrophage/microglial reaction caudal to a spinal transection in adult zebrafish. J. Comp. Neurol. 433 (1), 131–147. https://doi.org/10.1002/cne.1131.

Brann, J.H., Firestein, S.J., 2014. A lifetime of neurogenesis in the olfactory system. Front. Neurosci. 8, 182. https://doi.org/10.3389/fnins.2014.00182.

Brown, G.C., Neher, J.J., 2012. Eaten alive! Cell death by primary phagocytosis: 'phagoptosis.'. Trends Biochem. Sci. 37 (8), 325–332. https://doi.org/10.1016/J.TIBS.2012.05.002.

Bruttger, J., Karram, K., Wörtge, S., Regen, T., Marini, F., Hoppmann, N., Klein, M., Blank, T., et al., 2015. Genetic cell ablation reveals clusters of local self-renewing microglia in the mammalian central nervous system. Immunity 43 (1), 92–106. https://doi.org/10.1016/J.IMMUNI.2015.06.012.

Byrd, C.A., Brunjes, P., 2001. Neurogenesis in the olfactory bulb of adult zebrafish. Neuroscience 105 (4), 793–801. https://doi.org/10.1016/S0306-4522(01)00215-9.

Byrd, C.A., 2000. Deafferentation-induced changes in the olfactory bulb of adult zebrafish. Brain Res. 866 (1–2), 92–100. https://doi.org/10.1016/S0006-8993(00)02252-6.

Cacialli, P., Palladino, A., Lucini, C., 2018. Role of brain-derived neurotrophic factor during the regenerative response after traumatic brain injury in adult zebrafish. Neural Regen. Res. 13 (6), 941. https://doi.org/10.4103/1673-5374.233430.

Calvo, C.F., Yoshirnura, T., Gelrnan, M., Mallat, M., 1996. Production of monocyte chemotactic protein-1 by rat brain macrophages. Eur. J. Neurosci. 8 (8), 1725–1734. https://doi.org/10.1111/j.1460-9568.1996.tb01316.x.

Carrillo, S.A., Anguita-Salinas, C., Peña, O.A., Morales, R.A., Muñoz-Sánchez, S., Muñoz-Montecinos, C., Parees-Zuniga, S., Tapia, K., et al., 2016. Macrophage recruitment contributes to regeneration of mechanosensory hair cells in the zebrafish lateral line. J. Cell. Biochem. 117 (8), 1880–1889. https://doi.org/10.1002/jcb.25487.

Craig, S.E., Calinescu, A.A., Hitchcock, P.F., 2008. Identification of the molecular signatures integral to regenerating photoreceptors in the retina of the zebra fish. J. Ocul. Biol. Dis. Infor. 1 (2-4), 73. https://doi.org/10.1007/s12177-008-9011-5.

Davalos, D., Grutzendler, J., Yang, G., Kim, J.V., Zuo, Y., Jung, S., Littman, D.R., Dustin, M.L., et al., 2005. ATP mediates rapid microglial response to local brain injury in vivo. Nat. Neurosci. 8 (6), 752–758. https://doi.org/10.1038/nn1472.

David, S., Kroner, A., 2011. Repertoire of microglial and macrophage responses after spinal cord injury. Nat. Rev. Neurosci. 12 (7), 388–399. https://doi.org/10.1038/nrn3053.

de Preux Charles, A.-S., Bise, T., Baier, F., Marro, J., Jaźwińska, A., 2016. Distinct effects of inflammation on preconditioning and regeneration of the adult zebrafish heart. Open Biol. 6 (7), 160102. https://doi.org/10.1098/rsob.160102.

Ginhoux, F., Greter, M., Leboeuf, M., Nandi, S., See, P., Gokhan, S., Mehler, M.F., Conway, S.J., et al., 2010. Fate Mapping analysis reveals that adult microglia derive from primitive macrophages. Science 330 (6005), 841–845. https://doi.org/10.1126/science.1194637.

Gomez-Nicola, D., Perry, V.H., 2015. Microglial dynamics and role in the healthy and diseased brain. Neuroscientist 21 (2), 169–184. https://doi.org/10.1177/1073858414530512.

Grandel, H., Kaslin, J., Ganz, J., Wenzel, I., Brand, M., 2006. Neural stem cells and neurogenesis in the adult zebrafish brain: origin, proliferation dynamics, migration and cell fate. Dev. Biol. 295 (1), 263–277. https://doi.org/10.1016/J.YDBIO.2006.03.040.

Harry, G.J., Kraft, A.D., 2012. Microglia in the developing brain: a potential target with lifetime effects. NeuroToxicology 33 (2), 191–206. https://doi.org/10.1016/J.NEURO.2012.01.012.

Herbomel, P., Thisse, B., Thisse, C., 1999. Ontogeny and behaviour of early macrophages in the zebrafish embryo. Development 126 (17), 3735–3745.

Herbomel, P., Thisse, B., Thisse, C., 2001. Zebrafish early macrophages colonize cephalic mesenchyme and developing brain, retina, and epidermis through a M-CSF receptor-dependent invasive process. Dev. Biol. 238 (2), 274–288. https://doi.org/10.1006/DBIO.2001.0393.

Hong, S., Dissing-Olesen, L., Stevens, B., 2016. New insights on the role of microglia in synaptic pruning in health and disease. Curr. Opin. Neurobiol. 36, 128–134. https://doi.org/10.1016/j.conb.2015.12.004.

Inman, K.E., Downs, K.M., 2007. The murine allantois: emerging paradigms in development of the mammalian umbilical cord and its relation to the fetus. Genesis 45 (5), 237–258. https://doi.org/10.1002/dvg.20281.

Iqbal, T., Byrd-Jacobs, C., 2010. Rapid degeneration and regeneration of the zebrafish olfactory epithelium after triton X-100 application. Chem. Senses 35 (5), 351–361. https://doi.org/10.1093/chemse/bjq019.

Jonas, R.A., Yuan, T.F., Liang, Y.X., Jonas, J.B., Tay, D.K., Ellis-Behnke, R.G., 2012. The spider effect: morphological and orienting classification of microglia in response to stimuli in vivo. PLoS One 7 (2), 30763.

Kumar, A., Loane, D.J., 2012. Neuroinflammation after traumatic brain injury: opportunities for therapeutic intervention. Brain Behav. Immun. 26 (8), 1191–1201. https://doi.org/10.1016/J.BBI.2012.06.008.

Lawson, L.J., Perry, V.H., Dri, P., Gordon, S., 1990. Heterogeneity in the distribution and morphology of microglia in the normal adult mouse brain. Neuroscience 39 (1), 151–170. Retrieved from. http://www.ncbi.nlm.nih.gov/pubmed/2089275.

Lawson, L.J., Perry, V.H., Gordon, S., 1992. Turnover of resident microglia in the normal adult mouse brain. Neuroscience 48 (2), 405–415. Retrieved from. http://www.ncbi.nlm.nih.gov/pubmed/1603325.

März, M., Schmidt, R., Rastegar, S., Strähle, U., 2011. Regenerative response following stab injury in the adult zebrafish telencephalon. Dev. Dyn. 240 (9), 2221–2231. https://doi.org/10.1002/dvdy.22710.

McCarthy, G.F., Leblond, C.P., 1988. Radioautographic evidence for slow astrocyte turnover and modest oligodendrocyte production in the corpus callosum of adult mice infused with3H-thymidine. J. Comp. Neurol. 271 (4), 589–603. https://doi.org/10.1002/cne.902710409.

Missinato, M.A., Saydmohammed, M., Zuppo, D.A., Rao, K.S., Opie, G.W., Kühn, B., Tsang, M., 2018. Dusp6 attenuates Ras/MAPK signaling to limit zebrafish heart regeneration. Development 145 (5). https://doi.org/10.1242/dev.157206. dev157206.

Mittelbronn, M., Dietz, K., Schluesener, H.J., Meyermann, R., 2001. Local distribution of microglia in the normal adult human central nervous system differs by up to one order of magnitude. Acta Neuropathol. 101 (3), 249–255. https://doi.org/10.1007/s004010000284.

Morrison, H.W., Filosa, J.A., 2013. A quantitative spatiotemporal analysis of microglia morphology during ischemic stroke and reperfusion. J. Neuroinflammation 10 (1), 782. https://doi.org/10.1186/1742-2094-10-4.

Murray, P.J., Wynn, T.A., 2011. Protective and pathogenic functions of macrophage subsets. Nat. Rev. Immunol. 11 (11), 723–737. https://doi.org/10.1038/nri3073.

Nimmerjahn, A., Kirchhoff, F., Helmchen, F., 2005. Resting microglial cells are highly dynamic surveillants of brain parenchyma in vivo. Science 308 (5726), 1314–1318. https://doi.org/10.1126/science.1110647.

Paskin, T.R., Iqbal, T.R., Byrd-Jacobs, C.A., 2011. Olfactory bulb recovery following reversible deafferentation with repeated detergent application in the adult zebrafish. Neuroscience 196, 276–284.

Paskin, T.R., Byrd-Jacobs, C.A., 2012. Reversible deafferentation of the adult zebrafish olfactory bulb affects glomerular distribution and olfactory-mediated behavior. Behav. Brain Res. 235 (2), 293–301.

Peri, F., Nüsslein-Volhard, C., 2008. Live imaging of neuronal degradation by microglia reveals a role for v0-ATPase a1 in phagosomal fusion in vivo. Cell 133 (5), 916–927. https://doi.org/10.1016/J.CELL.2008.04.037.

Pozzuto, J.M., Fuller, C.L., Byrd-Jacobs, C.A., 2019. Deafferentation-induced alterations in mitral cell dendritic morphology in the adult zebrafish olfactory bulb. J. Bioenerg. Biomembr. 51 (1), 29–40.

Ransohoff, R.M., Perry, V.H., 2009. Microglial physiology: unique stimuli, specialized responses. Annu. Rev. Immunol. 27 (1), 119–145. https://doi.org/10.1146/annurev.immunol.021908.132528.

Ravichandran, K.S., Lorenz, U., 2007. Engulfment of apoptotic cells: signals for a good meal. Nat. Rev. Immunol. 7 (12), 964–974. https://doi.org/10.1038/nri2214.

Raymond, P.A., Barthel, L.K., Bernardos, R.L., Perkowski, J.J., 2006. Molecular characterization of retinal stem cells and their niches in adult zebrafish. BMC Dev. Biol. 6 (1), 36. https://doi.org/10.1186/1471-213X-6-36.

Reemst, K., Noctor, S.C., Lucassen, P.J., Hol, E.M., 2016. The indispensable roles of microglia and astrocytes during brain development. Front. Hum. Neurosci. 10, 566. https://doi.org/10.3389/fnhum.2016.00566.

Savill, J., Dransfield, I., Gregory, C., Haslett, C., 2002. A blast from the past: clearance of apoptotic cells regulates immune responses. Nat. Rev. Immunol. 2 (12), 965–975. https://doi.org/10.1038/nri957.

Schafer, D.P., Lehrman, E.K., Kautzman, A.G., Koyama, R., Mardinly, A.R., Yamasaki, R., Ransohoff, R.M., Greenberg, M.E., 2012. Microglia sculpt postnatal neural circuits in an activity and complement-dependent manner. Neuron 74 (4), 691–705. https://doi.org/10.1016/J.NEURON.2012.03.026.

Scheib, J.J., Pozzuto, J.M., Byrd-Jacobs, C.A., 2019. Reversible deafferentation of the zebrafish olfactory bulb with wax plug insertion. J. Neurosci. Methods 311 (1), 47–56. https://doi.org/10.1016/j.jneumeth.2018.10.014.

Shechter, R., Miller, O., Yovel, G., Rosenzweig, N., London, A., Ruckh, J., Kim, K.W., Klein, E., et al., 2013. Recruitment of beneficial M2 macrophages to injured spinal cord is orchestrated by remote brain choroid plexus. Immunity 38 (3), 555–569. https://doi.org/10.1016/J.IMMUNI.2013.02.012.

Shimizu, Y., Ueda, Y., Ohshima, T., 2018. Wnt signaling regulates proliferation and differentiation of radial glia in regenerative processes after stab injury in the optic tectum of adult zebrafish. Glia 66 (7), 1382–1394. https://doi.org/10.1002/glia.23311.

Silverman, S.M., Kim, B.-J., Howell, G.R., Miller, J., John, S.W.M., Wordinger, R.J., Clark, A.F., 2016. C1q propagates microglial activation and neurodegeneration in the visual axis following retinal ischemia/reperfusion injury. Mol. Neurodegener. 11 (1), 24. https://doi.org/10.1186/s13024-016-0089-0.

Streit, W.J., Heiko, A.E., Ae, B., Xue, Q.-S., 2009. Dystrophic (senescent) rather than activated microglial cells are associated with tau pathology and likely precede neurodegeneration in Alzheimer's disease. Acta Neuropathol. 118 (4), 475–485. https://doi.org/10.1007/s00401-009-0556-6.

Tremblay, M.-È., Lowery, R.L., Majewska, A.K., 2010. Microglial interactions with synapses are modulated by visual experience. PLoS Biol. 8 (11), e1000527. https://doi.org/10.1371/journal.pbio.1000527.

Tsarouchas, T.M., Wehner, D., Cavone, L., Munir, T., Keatinge, M., Lambertus, M., Underhill, A., Barret, T., et al., 2018. Dynamic control of proinflammatory cytokines Il-1β and Tnf-α by macrophages is necessary for functional spinal cord regeneration in zebrafish. Nature Communication 9 (1), 4670. https://doi.org/10.1038/s41467-018-07036-w.

van Ham, T.J., Brady, C.A., Kalicharan, R.D., Oosterhof, N., Kuipers, J., Veenstra-Algra, A., Sjollema, K.A., Peterson, R.T., et al., 2014v. Intravital correlated microscopy reveals differential macrophage and microglial dynamics during resolution of neuroinflammation. Dis. Model. Mech. 7 (7), 857–869. https://doi.org/10.1242/dmm.014886.

Vankirk, A.M., Byrd, C.A., 2003. Apoptosis following peripheral sensory deafferentation in the olfactory bulb of adult zebrafish. J. Comp. Neurol. 455 (4), 488–498.

Varvel, N.H., Grathwohl, S.A., Baumann, F., Liebig, C., Bosch, A., Brawek, B., Thal, D.R., Charo, I.F., et al., 2012. Microglial repopulation model reveals a robust homeostatic process for replacing CNS myeloid cells. Proc. Natl. Acad. Sci. U.S.A. 109 (44), 18150–18155. https://doi.org/10.2307/41829822.

Villanueva, R., Byrd-Jacobs, C.A., 2009. Peripheral sensory deafferentation affects olfactory bulb neurogenesis in zebrafish. Brain Res. 1269 (7), 31–39. https://doi.org/10.1016/j.brainres.2009.03.005.

Wattananit, S., Tornero, D., Graubardt, N., Memanishvili, T., Monni, E., Tatarishvili, J., Miskintye, G., Ge, R., et al., 2016. Monocyte-derived macrophages contribute to spontaneous long-term functional recovery after stroke in mice. J. Neurosci. 36 (15), 4182–4195. https://doi.org/10.1523/JNEUROSCI.4317-15.2016.

White, E.J., Kounelis, S.K., Byrd-Jacobs, C.A., 2015. Plasticity of glomeruli and olfactory-mediated behavior in zebrafish following detergent lesioning of the olfactory epithelium. Neuroscience 284, 622–631. https://doi.org/10.1016/J.NEUROSCIENCE.2014.10.036.

Woodcock, T.M., Frugier, T., Nguyen, T.T., Semple, B.D., Bye, N., Massara, M., Savino, B., Besio, R., et al., 2017. The scavenging chemokine receptor ACKR2 has a significant impact on acute mortality rate and early lesion development after traumatic brain injury. PLoS One 12 (11), e0188305. https://doi.org/10.1371/journal.pone.0188305.